Effects of force-field adaptation on neural activation and resting-state functional connectivity

Andria J. Farrens,[1] Andrea Zonnino,[1] and Fabrizio Sergi[1]

***Abstract*— Our group recently developed a novel fMRI-compatible wrist robot, the MR-SoftWrist, to study the neural processes that underlie force-field adaptation. Here we present our first fMRI pilot study on four healthy subjects. Our study validates the MR-SoftWrist as a tool for investigating motor adaptation of wrist pointing movements during fMRI and establishes neural activations associated with active motor control and off-line neural processing in three dynamic conditions.**

I. INTRODUCTION

Neuromotor adaptation is a common framework used to study motor learning [1]. While the behavioral effects of motor adaptation have been extensively studied, its neural correlates are much less understood. The neural correlates of motor adaptation can be derived using functional magnetic resonance imaging (fMRI). Task-based fMRI acquired during subject interaction with a novel force field can localize neural activity associated with active motor adaptation processes [2]. Resting state fMRI, acquired pre- and post-motor adaptation, can measure interactions between distinct brain regions following motor learning that reflect off-line motor learning processes [3]. Due to restrictions imposed by MRI compatibility, only a few previous studies have investigated the neural correlates of adaptation in response to dynamic perturbations. Moreover, previous dynamic adaptation studies used tasks that required shoulder/elbow rotations that may introduce movement-related confounds to fMRI.

We have recently developed an fMRI-compatible robot, the MR-SoftWrist, that allows application of fMRI to the study of motor adaptation to force perturbations during wrist pointing, a task that can be executed without causing fMRI image degradation. Here, we present the results of our first fMRI pilot study on four healthy subjects where we establish the neural correlates of motor adaptation to force perturbations and the ensuing off-line neural processes following interaction with the MR-SoftWrist.

II. METHODS

A. MR-SoftWrist

The MR-SoftWrist (Fig. 1, top left) supports wrist rotations about two axes, wrist flexion-extension (FE) and radial-ulnar deviation (RUD), in a circular workspace with a radius of 20 deg. The MR-SoftWrist has a maximum output torque of 1.5 N·m provided by piezoelectric ultrasonic motors, and measures end-effector force, velocity and position at a rate of 100 Hz. For an in-depth description of its design and control see [4], and for its fMRI compatibility see [5].

B. Experimental protocol

We adapted the standard force-field reaching task [1] to wrist pointing. Subjects held the handle of the MR-SoftWrist with their dominant (right) hand to control a cursor displayed on a monitor that was visible to the subject during fMRI. FE of the wrist moved the cursor horizontally, while RUD moved the cursor vertically. Rotation about the radio-ulnar axis was prevented by a custom support. Subjects were cued to make alternating FE rotations to move the cursor along a straight path to one of two targets, placed at (±12, 0) degrees in FE, RUD respectively. Subjects performed wrist pointing under three conditions: a no-force (NF), a resistive force (RF), and a counter-clockwise force (CF) (Fig. 1, top right). In the NF condition, the robot measured baseline performance with minimal interaction forces. In the RF and CF conditions, the robot applied a velocity-dependent torque, $\tau = B\dot{\theta}$, where $\tau = [\tau_{FE}, \tau_{RUD}]$, is proportional to the measured velocity $\dot{\theta} = [\dot{\theta}_{FE}, \dot{\theta}_{RUD}]$. In the RF mode, $B = [-2.5, 0; 0, -2.5]$ mN·m·s/deg, effectively increasing the impedance in the direction of movement. In the CF mode, $B = [0, 2.5; -2.5, 0]$ mN·m·s/deg, resulting in perturbations lateral to the direction of movement. In all conditions, error-clamp trials placed with a $1/8^{th}$ probability sampled subject generated force profiles without disrupting adaptation [1].

Our protocol is reported in Fig. 1, bottom. Task conditions were 6 blocks of 24 trials, with 15 sec. breaks between blocks. FMRI data were collected on a 3-T Siemens scanner, 64-channel head coil, 2x2x2 mm resolution, and 1 sec. TR.

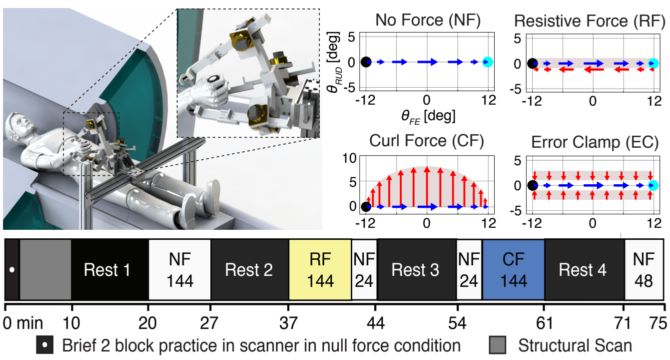

Fig. 1. Top left: MR-SoftWrist in its operating condition. Top right: Task-specific force-fields; robot applied force in red, cursor velocity blue. Bottom: fMRI task design. Number of trials are listed beneath each active block title.

*Work supported by the AHA Scientist Development Grant 17SDG33690002, by the University of Delaware Research Foundation grant no. 16A01402, by the ACCEL NIGMS IDeA grant U54-GM104941.

[1] Human Robotics Lab, Department of Biomedical Engineering, University of Delaware, Newark, DE USA. afarrens@udel.edu, zonni@udel.edu, fabs@udel.edu

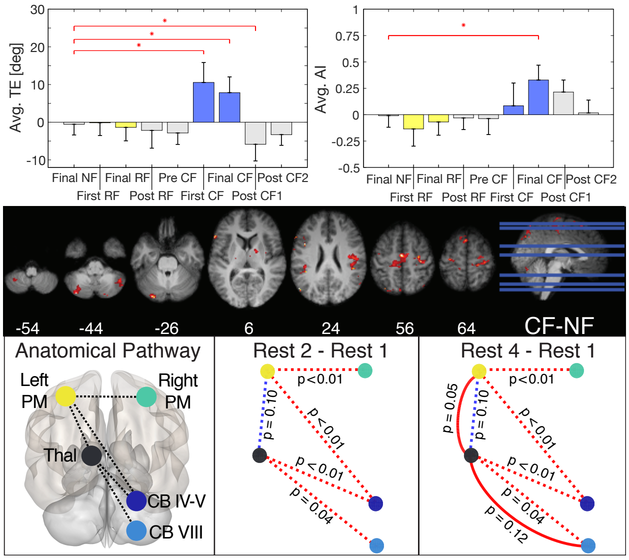

Fig. 2. Top: Comparison of whole-group mean TE and AI, averaged across single blocks of each training condition. Middle: Axial slices of CF-NF group contrast map ($p_{unc} < 0.025$). Bottom: Regions included in CTC rsFC analysis. Dashed lines: baseline rsFC; Curved lines: change in rsFC; Red: increased/positive correlation; Blue: decreased/anti-correlation.

C. Data Analysis

1) Behavioral: Trial performance was quantified via trajectory error (TE), defined as the internal angle between the line connecting the cursor at maximal velocity to the start target to the end target (counter-clockwise positive). To quantify change in force production, we defined an adaptation index (AI) as the beta weight, β_1, of the measured force profile during EC trials regressed on to the ideal compensatory curl-force profile: $F_{actual}(t) = \beta_1 F_{ideal}(t) + \beta_0(t) + \varepsilon(t)$ [6]. We used one-way repeated measures ANOVAs to assess the effects of control mode (NF, RF, CF) on TE and AI.

2) fMRI data: All fMRI data were realigned and normalized into standard (MNI) space for group analysis. We used a block design to investigate the effect of each active condition (NF, RF, and CF) on neural activity, and included head motion parameters as regressors of no interest (all movement < 1 mm). To investigate the neural activity associated with adaptation, we preformed contrasts between conditions CF and NF. Contrast between conditions CF and RF served as a secondary control for neural activity associated with force.

Interactions between distinct brain regions at rest were investigated using resting state functional connectivity (rsFC) analysis, defined as the correlation of fMRI signal measured in one brain region to another. Due to our small sample size, we restricted our rsFC analysis to regions within the cortico-thalamic-cerebellar (CTC) network, previously implicated in motor learning and adaptation (Fig. 2, bottom) [1]. Comparison of baseline rsFC (Rest 1) and rsFC measured after each active mode assessed short-term changes in rsFC associated with off-line processing of force-field training.

III. RESULTS

A. Behavioral Metrics

Analysis of TE and AI showed characteristic effects of motor adaptation (Fig. 2, top). The one-way ANOVA showed a significant effect of control mode on both TE and AI ($p < 0.001$). A post-hoc Tukey HSD test showed TE in the CF mode was significantly greater compared to the RF and NF modes ($e_{NF} = -0.81 \pm 2.96$ deg, $e_{RF} = -0.70 \pm 3.43$ deg, $e_{CF} = 8.01 \pm 4.97$ deg). TE in the NF block immediately following the CF mode was significantly more negative than in the initial NF block, confirming the presence of after-effects ($e_{postCF} = -5.86 \pm 4.41$ deg). Post-hoc analysis of AI showed a significant effect of the CF mode on AI, indicative of adaptation ($AI_{NF} = .01 \pm .11, AI_{CF} = .33 \pm .14$).

B. fMRI Analysis

In all conditions, activations were localized predominantly in the left primary motor cortex (PM), left thalamus (Thal) and right cerebellum (CB) V and CB VIII, in line with current knowledge on motor control. Significant activation was also detected contralaterally to these regions. The contrast between CF and NF modes showed greater activation in the right and left PM cortices, Thal, and CB V, which suggests that task execution under lateral perturbations requires greater involvement of bilateral motor areas (Fig. 2, middle). The contrast between CF and RF modes—meant to isolate the effects of adaptation in matched force conditions—showed greater activation in the right PM and left CB, which suggests a greater involvement of the non-dominant cortico-cerebellar pathway for lateral perturbations (adaptation).

Comparison of baseline to post-adaptation rsFC (Rest 4-Rest 1) showed increased rsFC between the PM and Thal ($p = 0.05$), and the Thal and CB VIII ($p = 0.12$) (Fig. 2, bottom). No significant change was measured in the post-NF mode (Rest 2-Rest 1), suggesting the changes may be unique to off-line motor learning processes following adaptation.

IV. CONCLUSIONS

Our behavioral results validate the MR-Softwrist as a tool to study motor adaptation of wrist pointing during fMRI. Our fMRI results show significant activation in brain regions previously inferred to be associated with motor adaptation and establish preliminary changes in rsFC following adaptation.

REFERENCES

[1] R. Shadmehr. Learning to Predict and Control the Physics of Our Movements. *The Journal of Neuroscience*, 37(7):1663–1671, 2017.

[2] J. Diedrichsen. Neural Correlates of Reach Errors. *J. Neurosci*, 25(43):9919–9931, 2005.

[3] S. Sami, E. M. Robertson, and R. C. Miall. The Time Course of Task-Specific Memory Consolidation Effects in Resting State Networks. *J. Neurosci*, 34(11):3982–3992, 2014.

[4] A. Erwin, M. K. O Malley, D. Ress, and F. Sergi. Development , Control , and MRI-Compatibility of the MR-SoftWrist. *IEEE ICORR*, pages pp. 187–192, 2015.

[5] A. J. Farrens and et. al. Quantitative Testing of fMRI-compatibility of an Electrically Active Mechatronic Device for Robot-Assisted Sensorimotor Protocols. *IEEE Trans. on Biomed Eng*, pages 1–13, 2017.

[6] W. M. Joiner and M. A. Smith. Long-term retention explained by a model of short-term learning in the adaptive control of reaching. *J. Neurophysiol*, 100(5):2948–55, 2008.